Transient diffusion in a tube with dead ends

Leonardo Dagdug[a)]
Departamento de Fisica, Universidad Autonoma Metropolitana-Iztapalapa, 09340 Mexico DF, Mexico

Alexander M. Berezhkovskii
Mathematical and Statistical Computing Laboratory, Division for Computational Bioscience, Center for Information Technology, National Institutes of Health, Bethesda, Maryland 20892, USA

Yurii A. Makhnovskii
Topchiev Institute of Petrochemical Synthesis, Russian Academy of Sciences, Leninsky Prospect 29, 119991 Moscow, Russia

Vladimir Yu. Zitserman
Joint Institute for High Temperatures, Russian Academy of Sciences, 13/19 Ul. Izhorskaya, 125412 Moscow, Russia

(Received 31 August 2007; accepted 12 October 2007; published online 14 December 2007)

A particle diffusing in a tube with dead ends, from time to time enters a dead end, spends some time in the dead end, and then comes back to the tube. As a result, the particle spends in the tube only a part of the entire observation time that leads to slowdown of its diffusion along the tube. We study the transient diffusion in a tube with periodic identical dead ends formed by cavities of volume V_{cav} connected to the tube by cylindrical channels of length L and radius a, which is assumed to be much smaller than the tube radius R and the distance l between neighboring dead ends. Assuming that the particle initial position is uniformly distributed over the tube, we analyze the monotonic decrease of the particle diffusion coefficient $D(t)$ from its initial value $D(0)=D$, which characterizes diffusion in the tube without dead ends, to its asymptotic long-time value $D(\infty)=D_{eff}<D$. We derive an expression for the Laplace transform of $D(t)$, denoted by $\hat{D}(s)$, where s is the Laplace parameter. Although the expression is too complicated to be inverted analytically, we use it to find the relaxation time of the process as a function of the geometric parameters of the system mentioned above. To check the accuracy of our results, we ran Brownian dynamics simulations and found the mean squared displacement of the particle as a function of time by averaging over 5×10^4 realizations of the particle trajectory. The time-dependent mean squared displacement found in simulations is compared with that obtained by numerically inverting the Laplace transform of the mean squared displacement predicted by the theory, which is given by $2\hat{D}(s)/s$. Comparison shows excellent agreement between the two time dependences that support the approximations used when developing the theory. © *2007 American Institute of Physics*. [DOI: 10.1063/1.2805068]

I. INTRODUCTION

This paper deals with diffusion of a particle in a tube with periodic identical dead ends separated by the distance l, as shown in Fig. 1. A dead end is formed by a cavity of volume V_{cav} connected to the tube by a cylindrical channel of length L and radius a. The presence of dead ends slows down the diffusion along the tube compared to that in the ordinary tube. This happens because the particle interrupts its motion along the tube when it enters in a dead end. The major focus of this paper is on the transient behavior of the diffusion coefficient $D(t)$, assuming that the particle is in the tube at $t=0$, and the distribution of its initial position is uniform over the tube. As t goes from zero to infinity, $D(t)$ monotonically decreases from D to D_{eff}, where D is the particle diffusion constant in the tube without dead ends and D_{eff} is the effective diffusion constant in the tube with dead ends. While it is easy to find D_{eff}, analysis of the transient behavior of $D(t)$ is a much more complicated problem.

Effect of dead ends on diffusion has been discussed when analyzing diffusive transport in different biological processes. Examples include transport in dendrites,[1,2] extracellular diffusion in brain tissue,[3–7] and intratissue diffusion of water and other substances in muscle.[8–10] Another field, where dead ends play an important role, is diffusive transport

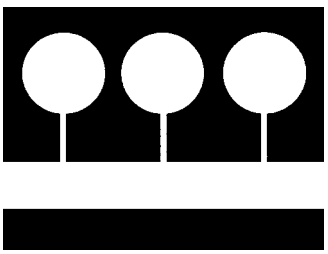

FIG. 1. A tube with identical dead ends located at regular intervals. A dead end is formed by a cavity connected to the tube by a narrow channel.

a)Electronic mail: ldagdug@helix.nih.gov.

in soil.[11–14] The first approximate theory of non-steady-state diffusion in a linear porous medium with dead ends was suggested by Goodknight *et al.*[15] We discuss the relation between our approach to the problem and that by Goodnight *et al.* in Section V. A rigorous formulation of the theory based on the eigenfunction expansion was suggested by Sen *et al.*[16] To find the eigenfunctions, one has to solve the eigenvalue problem in three dimensions. Unfortunately, for a tube with dead ends, this problem is unsolvable because of the geometrical complexity. In the theory developed in this paper, we suggest a new approximate approach which allows us to overcome the difficulties.

Our analysis is based on the assumption that the channel radius is small compared to the tube radius R and the distance l, $a \ll R, l$, while L and V_{cav} can be arbitrary. We define the time-dependent diffusion coefficient for a particle initially at $x=x_0$, $D(t|x_0)$, in terms of the mean squared displacement of this particle along the tube, $\langle \Delta x^2(t|x_0)\rangle$. This quantity linearly grows with time when the particle is in the tube and does not change when the particle is in a dead end. Introducing the probability of finding the particle in the tube at time t, $P(t|x_0)$, we can write

$$D(t|x_0) = \frac{1}{2}\frac{d\langle \Delta x^2(t|+x_0)\rangle}{dt} = DP(t|x_0). \tag{1.1}$$

The probability $P(t|x_0)$ varies from unity at $t=0$, $P(0|x_0)=1$, to its equilibrium value as $t\to\infty$, $P(\infty|x_0)=P_{eq}$,

$$P(\infty|x_0) = P_{eq} = \frac{V_{tube}}{V_{tube}+V_{de}}, \tag{1.2}$$

where V_{tube} and V_{de} are volumes of the tube and the dead end given by $V_{tube}=\pi R^2 l$ and $V_{de}=V_{ch}+V_{cav}$ with the channel volume $V_{ch}=\pi a^2 L$. Respectively, $D(t|x_0)$ is equal to D at $t=0$ and D_{eff},

$$D_{eff} = DP_{eq} = D\frac{V_{tube}}{V_{tube}+V_{de}}, \tag{1.3}$$

as $t\to\infty$.

Thus, the problem of finding $D(t|x_0)$ is reduced to that of finding probability $P(t|x_0)$. To calculate $D(t)$, we have to average $D(t|x_0)$ over x_0,

$$D(t) = \frac{1}{l}\int_{-l/2}^{l/2} D(t|x_0)dx_0 = DP(t), \tag{1.4}$$

where $P(t)$ is the probability of finding the particle in the tube at time t averaged over the particle initial position x_0,

$$P(t) = \frac{1}{l}\int_{-l/2}^{l/2} P(t|x_0)dx_0. \tag{1.5}$$

One of the main results of this paper is an exact solution for the Laplace transform of $P(t)$. This transform is too complicated to be inverted analytically. Nevertheless, we use it to find a relaxation time τ_{rel} that provides a natural time scale characterizing relaxation of $D(t)$ from D to D_{eff}. We derive an expression which gives τ_{rel} as a function of the geometric parameters, a, R, l, L, and V_{cav}, as well as the particle diffusion constants in the tube and in the channel, D_{ch}, which may be much smaller than D. It is assumed that the particle diffusion constant in the cavity is equal to that in the tube.

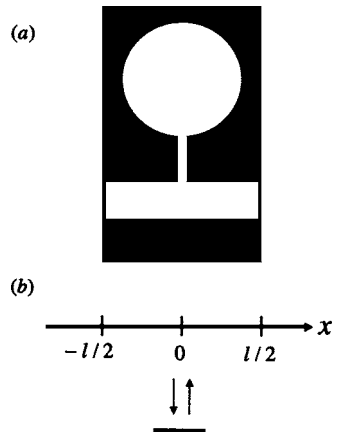

FIG. 2. A unit cell of the periodic structure shown in Fig. 1 with reflecting boundaries at the ends of the cell (panel a) and the equivalent 1D problem with a reversible binding site representing the dead end (panel b).

The outline of the paper is as follows. Main general results of our analysis are presented in the next section. In Sec. III, we introduce the relaxation function and use it to find the relaxation time. Illustrative examples are discussed in Sec. IV. In this section, we show that our theoretical predictions are in excellent agreement with the results obtained in Brownian dynamics simulations. This supports the approximations, which we use when developing the theory. In Sec. V, we discuss the relation between our approach and the Goodnight-Klikoff-Fatt (GKF) approach proposed in Ref. 15. We show that the GKF approach is a particular case of the more general approach proposed in this paper and indicate the conditions of its applicability. A summary of this study is given in the last section.

II. GENERAL RESULTS

In this section, we present our general results and outline their derivation. Because the system under consideration is periodic, we can analyze the probability $P(t|x_0)$ by considering the particle motion within a unit cell of the periodic structure with reflecting boundaries at its ends, as shown in Fig. 2(a). The problem is too complicated to be solved analytically by means of conventional methods of mathematical physics[16] because of the nontrivial three-dimensional (3D) geometry. A key step of our analysis, which allows us to solve the problem, is a replacement of the unsolvable 3D problem by an equivalent one-dimensional (1D) problem, shown in Fig. 2(b), that can be solved with relative ease.

The equivalent problem describes the particle motion in the tube as 1D diffusion in the x direction on an interval of length l with reflecting endpoints. The dead end is modeled as a reversible binding site located in the center of the interval. Entrance on the site is described by a delta sink of the amplitude κ,

$$\kappa = \frac{4Da}{\pi R^2}, \tag{2.1}$$

in the 1D diffusion equation.[17] After spending some time in the dead end the particle returns to the tube. The time spent

in the dead end is a random variable. We describe its distribution by the probability density $\varphi_{de}(t)$. For the sake of convenience, we have placed the binding site at the origin, $x=0$, and the reflecting endpoints of the interval at $x=\pm l/2$.

Replacement of the initial 3D problem [Fig. 2(a)] by the equivalent 1D problem [Fig. 2(b)] is an approximation which is justified only on the condition that $a \ll R, l$. We discuss the approximations used in our analysis in detail at the end of this section. To validate the approximations, we ran Brownian dynamics simulations and found excellent agreement between the theoretical predictions and numerical results. This is discussed in Sec. IV.

We begin with establishing a relation between the Laplace transforms of the probabilities $P(t|x_0)$ and $P(t|0)$. The latter may be considered as the probability of finding a particle in the tube at time t after it escaped from the dead end at $t=0$. To find the relation, we introduce the probability density for the first passage time from x_0 to the origin, $w(t|x_0)$, and the probability that the particle, initially at x_0, has never touched the origin for time t, $W(t|x_0)$,

$$W(t|x_0) = \int_t^\infty w(t'|x_0)dt'. \tag{2.2}$$

We use these two functions to write the integral equation which relates $P(t|x_0)$ and $P(t|0)$,

$$P(t|x_0) = W(t|x_0) + \int_0^t P(t-t'|0)w(t'|x_0)dt'. \tag{2.3}$$

Laplace transforming this equation and using the relation

$$\hat{W}(s|x_0) = \frac{1}{s}[1-\hat{w}(s|x_0)], \tag{2.4}$$

which follows from Eq. (2.2), we obtain

$$\hat{P}(s|x_0) = \frac{1}{s}[1-\hat{w}(s|x_0)] + \hat{w}(s|x_0)\hat{P}(s|0). \tag{2.5}$$

This allows us to find a relation between the Laplace transform of $P(t)$ defined in Eq. (1.5) and $\hat{P}(s|0)$ by averaging Eq. (2.5) over the starting position x_0,

$$\hat{P}(s) = \frac{1}{s}[1-\hat{w}(s|av)] + \hat{w}(s|av)\hat{P}(s|0), \tag{2.6}$$

where $\hat{w}(s|av)$ is the average of $\hat{w}(s|x_0)$,

$$\hat{w}(s|av) = \frac{1}{l}\int_{-l/2}^{l/2} \hat{w}(s|x_0)dx_0. \tag{2.7}$$

A derivation of $\hat{w}(s|av)$, outlined in Appendix A, leads to

$$\hat{w}(s|av) = \frac{2}{l}\sqrt{\frac{D}{s}}\tanh\left(\frac{l}{2}\sqrt{\frac{s}{D}}\right). \tag{2.8}$$

Function $\hat{P}(s|0)$ can be found by solving a two-state problem of the particle transitions between the tube and the dead end,

$$\text{tube} \rightleftarrows \text{dead end}. \tag{2.9}$$

In general, the transitions are non-Markovian and the probability densities for the particle lifetime in the tube $\varphi_{tube}(t)$ and in the dead end $\varphi_{de}(t)$ are not single exponentials. Derivations of $\hat{\varphi}_{tube}(s)$ and $\hat{\varphi}_{de}(s)$ outlined in Appendices B and C, respectively, lead to

$$\begin{aligned}\hat{\varphi}_{tube}(s) &= \frac{1}{1+\frac{2\sqrt{sD}}{\kappa}\tanh\left(\frac{l}{2}\sqrt{\frac{s}{D}}\right)} \\ &= \frac{1}{1+\frac{\pi R^2}{2a}\sqrt{\frac{s}{D}}\tanh\left(\frac{l}{2}\sqrt{\frac{s}{D}}\right)} \\ &= \frac{1}{1+\frac{V_{tube}}{4Da}s\hat{w}(s|av)}\end{aligned} \tag{2.10}$$

and

$$\hat{\varphi}_{de}(s) = \frac{(s+k_{cav})\cosh\left(L\sqrt{\frac{s}{D_{ch}}}\right) + \kappa_{ch}\sqrt{\frac{s}{D_{ch}}}\sinh\left(L\sqrt{\frac{s}{D_{ch}}}\right)}{(2s+k_{cav})\cosh\left(L\sqrt{\frac{s}{D_{ch}}}\right) + \kappa_{ch}\sqrt{\frac{s}{D_{ch}}}\left[1+\frac{D_{ch}}{\kappa_{ch}^2}(s+k_{cav})\right]\sinh\left(L\sqrt{\frac{s}{D_{ch}}}\right)}. \tag{2.11}$$

Here, k_{cav} and κ_{ch} are given by[18,19]

$$k_{cav} = \frac{4Da}{V_{cav}}, \quad \kappa_{ch} = \frac{4D}{\pi a}. \tag{2.12}$$

In Eq. (2.10), we have used the expression for κ given in Eq. (2.1).

According to the kinetic scheme in Eq. (2.9), the probability $P(t|0)$ satisfies the linear integral equation

$$P(t|0) = S_{tube}(t) + \int_0^t dt_1 \varphi_{tube}(t_1)\int_0^{t-t_1} P(t-t_1-t_2|0)\varphi_{de}(t_2)dt_2, \tag{2.13}$$

where we have introduced the particle survival probability in the tube $S_{tube}(t)$,

$$S_{\text{tube}}(t) = \int_t^\infty \varphi_{\text{tube}}(t')dt'. \tag{2.14}$$

Laplace transforming Eq. (2.13) and solving the resultant linear equation, we obtain

$$\hat{P}(s|0) = \frac{1 - \hat{\varphi}_{\text{tube}}(s)}{s[1 - \hat{\varphi}_{\text{tube}}(s)\hat{\varphi}_{\text{de}}(s)]}. \tag{2.15}$$

Finally, we use Eq. (1.4) and the results in Eqs. (2.6) and (2.15) to write the Laplace transform of the ratio $D(t)/D$ as

$$\frac{\hat{D}(s)}{D} = \hat{P}(s) = \frac{1}{s}\left\{1 - \hat{w}(s|av)\frac{\hat{\varphi}_{\text{tube}}(s)[1 - \hat{\varphi}_{\text{de}}(s)]}{1 - \hat{\varphi}_{\text{tube}}(s)\hat{\varphi}_{\text{de}}(s)}\right\}. \tag{2.16}$$

The Laplace transform in Eq. (2.16) is one of the main results of this paper. One can find transient behavior of $D(t)$ inverting this transform. The illustrative example discussed in Sec. IV shows that our theoretical predictions are in excellent agreement with the results obtained in Brownian dynamics simulations. In general, the transform can be inverted only numerically. However, one can use the transform to find the mean relaxation time, which provides a natural time scale that characterizes transition of $D(t)$ from D to D_{eff}. This is done in the next section.

The theory leading to the expression for $\hat{P}(s)$ in Eq. (2.16) has been developed in two steps. First, we establish an exact relation between $\hat{P}(s)$ and $\hat{P}(s|0)$ [Eq. (2.6)]. Then, we find an exact solution for $\hat{P}(s|0)$ [Eq. (2.15)] by analyzing the two-state problem [Eq. (2.9)], which leads to the integral equation in Eq. (2.13). The exact result in Eq. (2.16) is obtained when we substitute $\hat{P}(s|0)$ given in Eq. (2.15) into Eq. (2.6). The expression in Eq. (2.16) gives $\hat{P}(s)$ in terms of functions $\hat{w}(s)$, $\hat{\varphi}_{\text{tube}}(s)$, and $\hat{\varphi}_{\text{de}}(s)$ defined in Eqs. (2.8), (2.10), and (2.11), respectively. Only one of these three functions is an exact solution, namely, $\hat{w}(s)$ in Eq. (2.8). Three different approximations are used in Appendices B and C when deriving $\hat{\varphi}_{\text{tube}}(s)$ and $\hat{\varphi}_{\text{de}}(s)$ given in Eqs. (2.10) and (2.11). (i) When deriving $\hat{\varphi}_{\text{tube}}(s)$, we describe the entrance of a particle diffusing in the tube into a narrow connecting channel, $a \ll R, l$, by introducing a delta sink into the diffusion equation [Eq. (B1)]. (ii) We assume that the distribution of the particle lifetime in the cavity is single exponential and characterize this distribution by the rate constant k_{cav} given in Eq. (2.12). (iii) When analyzing the particle motion in the channel, we replace complex dynamics at the channel boundaries by the effective radiation boundary conditions [see Eqs. (C1)–(C3)], containing the rate constant κ_{ch} given in Eq. (2.12). These three approximations have been suggested and tested numerically in Refs. 17–19.

III. RELAXATION TIME

As $t \to \infty$, $P(t)$ and $D(t)$ approach their asymptotic values P_{eq} and D_{eff} given in Eqs. (1.2) and (1.3), respectively. One can see this from the small-s expansion of $\hat{P}(s)$ in Eq. (2.16),

$$P(\infty) = P_{\text{eq}} = \lim_{s\to 0} s\hat{P}(s) = \frac{\langle \tau_{\text{tube}} \rangle}{\langle \tau_{\text{tube}} \rangle + \langle \tau_{\text{de}} \rangle} = \frac{V_{\text{tube}}}{V_{\text{tube}} + V_{\text{de}}}, \tag{3.1}$$

where we have used the relations which we also use in our further analysis,

$$\hat{\varphi}_{\text{tube}}(s) \approx 1 - s\langle \tau_{\text{tube}} \rangle + \frac{s^2}{2}\langle \tau_{\text{tube}}^2 \rangle, \tag{3.2}$$

$$\hat{\varphi}_{\text{de}}(s) \approx 1 - s\langle \tau_{\text{de}} \rangle + \frac{s^2}{2}\langle \tau_{\text{de}}^2 \rangle, \tag{3.3}$$

$$\hat{w}(s|av) \approx 1 - s\langle \tau_w \rangle. \tag{3.4}$$

Here, $\langle \tau_{\text{tube}} \rangle$, $\langle \tau_{\text{tube}}^2 \rangle$ and $\langle \tau_{\text{de}} \rangle$, $\langle \tau_{\text{de}}^2 \rangle$ are the first and second moments of the particle lifetime in the tube and in the dead end, respectively, and $\langle \tau_w \rangle$ is the mean first passage time of the particle to the origin averaged over its starting positions. The last equality in Eq. (3.1) follows from the ergodicity of the particle dynamics as well as from the expressions for $\langle \tau_{\text{tube}} \rangle$ and $\langle \tau_{\text{de}} \rangle$, which can be obtained from Eqs. (2.10) and (2.11),

$$\langle \tau_{\text{tube}} \rangle = \frac{V_{\text{tube}}}{4Da} = \frac{\pi R^2 l}{4Da}, \quad \langle \tau_{\text{de}} \rangle = \frac{V_{\text{de}}}{4Da} = \frac{V_{\text{cav}} + \pi a^2 L}{4Da}. \tag{3.5}$$

It is convenient to describe the relaxation process by means of the relaxation function $R(t)$ given by

$$R(t) = \frac{D(t) - D_{\text{eff}}}{D - D_{\text{eff}}} = \frac{P(t) - P_{\text{eq}}}{1 - P_{\text{eq}}}. \tag{3.6}$$

This function monotonically decreases from unity to zero as t goes from zero to infinity. The relaxation time τ_{rel} can be defined in terms of $R(t)$ as

$$\tau_{\text{rel}} = \int_0^\infty R(t)dt = \hat{R}(s=0). \tag{3.7}$$

Here, $\hat{R}(s)$ is the Laplace transform of $R(t)$, which can be found by using the expression for $\hat{P}(s)$ in Eq. (2.16),

$$\hat{R}(s) = \frac{\hat{P}(s) - \frac{1}{s}P_{\text{eq}}}{1 - P_{\text{eq}}} = \frac{(1 - P_{\text{eq}})[1 - \hat{\phi}_{\text{tube}}(s)\hat{\varphi}_{\text{de}}(s)] - \hat{w}(s|av)\hat{\varphi}_{\text{tube}}(s)[1 - \hat{\varphi}_{\text{de}}(s)]}{s(1 - P_{\text{eq}})[1 - \hat{\varphi}_{\text{tube}}(s)\hat{\varphi}_{\text{de}}(s)]}. \tag{3.8}$$

Substituting the expansions in Eqs. (3.2)–(3.4) into Eq. (3.8) and taking the limit $s \to 0$, we obtain

$$\tau_{\rm rel}=\frac{\langle\tau_{\rm tube}\rangle\langle\tau_{\rm de}^2\rangle+2\langle\tau_{\rm de}\rangle\left[\langle\tau_{\rm tube}\rangle^2+\langle\tau_w\rangle(\langle\tau_{\rm tube}\rangle+\langle\tau_{\rm de}\rangle)-\frac{1}{2}\langle\tau_{\rm tube}^2\rangle\right]}{2\langle\tau_{\rm de}\rangle(\langle\tau_{\rm tube}\rangle+\langle\tau_{\rm de}\rangle)}. \tag{3.9}$$

Using Eq. (2.10), we find that

$$\langle\tau_{\rm tube}^2\rangle=2\langle\tau_{\rm tube}\rangle(\langle\tau_{\rm tube}\rangle+\langle\tau_w\rangle), \tag{3.10}$$

where the mean first passage time $\langle\tau_w\rangle$ is given by

$$\langle\tau_w\rangle=\frac{l^2}{12D}. \tag{3.11}$$

This can be obtained from the Laplace transform of the probability density $\hat{w}(s|av)$ in Eq. (2.8). The relation in Eq. (3.10) allows us to write Eq. (3.9) as

$$\tau_{\rm rel}=\frac{\langle\tau_{\rm tube}\rangle\langle\tau_{\rm de}^2\rangle+2\langle\tau_w\rangle\langle\tau_{\rm de}\rangle^2}{2\langle\tau_{\rm de}\rangle(\langle\tau_{\rm tube}\rangle+\langle\tau_{\rm de}\rangle)}. \tag{3.12}$$

Three out of the four moments entering into Eq. (3.12) are given in Eqs. (3.5) and (3.11). The unknown moment is the second moment of the particle lifetime in the dead end, $\langle\tau_{\rm de}^2\rangle$. It can be found from $\hat{\varphi}_{\rm de}(s)$ in Eq. (2.11). The result is

$$\langle\tau_{\rm de}^2\rangle=2\langle\tau_{\rm de}\rangle^2\left\{1+\left(\frac{V_{\rm cav}}{V_{\rm de}}\right)^2+\frac{4DL}{\pi D_{\rm ch}a}\left[\frac{V_{\rm cav}}{V_{\rm de}}+\frac{1}{3}\left(\frac{V_{\rm ch}}{V_{\rm de}}\right)^2\right]\right\}. \tag{3.13}$$

Thus, we can find $\tau_{\rm rel}$ as a function of the geometric parameters a, R, l, L, and $V_{\rm cav}$ and the diffusion constants D and $D_{\rm ch}$. This is another important result of this paper.

A. No connecting channels: $L=0$

In the absence of the connecting channel, $L=0$, transitions from the dead end to the tube are Markovian, and Eq. (3.13) simplifies and takes the form

$$\langle\tau_{\rm de}^2\rangle=4\langle\tau_{\rm de}\rangle^2. \tag{3.14}$$

As a consequence, Eq. (3.12) also simplifies and can be written as

$$\tau_{\rm rel}=\frac{\langle\tau_{\rm de}\rangle(2\langle\tau_{\rm tube}\rangle+\langle\tau_w\rangle)}{\langle\tau_{\rm tube}\rangle+\langle\tau_{\rm de}\rangle}=\frac{1}{2D}\left(\frac{V_{\rm tube}}{a}+\frac{l^2}{6}\right)\frac{V_{\rm cav}}{V_{\rm tube}+V_{\rm cav}}, \tag{3.15}$$

where we have used the expressions in Eqs. (3.5) and (3.11) for the times $\langle\tau_{\rm tube}\rangle$, $\langle\tau_{\rm de}\rangle$, and $\langle\tau_w\rangle$, respectively, and the fact that $V_{\rm de}=V_{\rm cav}$.

Capture of the particle diffusing in the tube by the dead ends can be characterized by the dimensionless parameter $\lambda=al/R^2$. When $\lambda\ll1$, time $\langle\tau_{\rm tube}\rangle$ is much greater than time $\langle\tau_w\rangle$, $\langle\tau_{\rm tube}\rangle\gg\langle\tau_w\rangle$, and the average distance passed by the particle between successive captures significantly exceeds distance l between neighboring dead ends. In this weak capture (wc) regime, the expression in Eq. (3.15) further simplifies and takes the form

$$\tau_{\rm rel}^{\rm (wc)}=\frac{1}{2Da}\frac{V_{\rm cav}V_{\rm tube}}{V_{\rm cav}+V_{\rm tube}}. \tag{3.16}$$

In the opposite, strong capture (sc) regime, $\lambda\gg1$, we have $\langle\tau_{\rm tube}\rangle\ll\langle\tau_w\rangle$, and a particle escaping from a dead end is recaptured by the same dead end with probability close to unity. In this regime, $\tau_{\rm rel}$ in Eq. (3.15) takes the form

$$\tau_{\rm rel}^{\rm (sc)}=\langle\tau_w\rangle\frac{V_{\rm cav}}{V_{\rm cav}+V_{\rm tube}}=\frac{l^2}{12D}\frac{V_{\rm cav}}{V_{\rm cav}+V_{\rm tube}}. \tag{3.17}$$

The relaxation kinetics significantly simplifies and becomes single exponential when $L=0$ and $\lambda\ll1$ (the weak capture regime). According to Eqs. (2.8), (2.10), and (2.11) in this case, we have

$$\hat{w}(s|av)\hat{\varphi}_{\rm tube}(s)\approx\hat{\varphi}_{\rm tube}(s)\approx\frac{k_{\rm tube}}{s+k_{\rm tube}}, \tag{3.18}$$

$$\hat{\varphi}_{\rm de}(s)=\frac{s+k_{\rm cav}}{2s+k_{\rm cav}}, \tag{3.19}$$

where we have introduced the rate constant $k_{\rm tube}$,

$$k_{\rm tube}=\frac{l}{\kappa}=\frac{V_{\rm tube}}{4Da}. \tag{3.20}$$

Substituting the expressions in Eqs. (3.18) and (3.19) into Eq. (3.8) we find that

$$\hat{R}(s)=\frac{1}{s+(k_{\rm tube}+k_{\rm cav})/2} \tag{3.21}$$

and, hence,

$$D(t)=D_{\rm eff}+(D-D_{\rm eff})\exp[-(k_{\rm tube}+k_{\rm cav})t/2]. \tag{3.22}$$

In this case, the transitions in the kinetic scheme [Eq. (2.9)] are Markovian with the rate constants given by $k(\text{tube}\to\text{cav})=k_{\rm tube}/2$ and $k(\text{cav}\to\text{tube})=k_{\rm cav}/2$. The expressions for $k(\text{tube}\to\text{cav})$ and $k(\text{cav}\to\text{tube})$ become obvious if one takes into account the fact that, sitting at the boundary separating a cavity and the tube, a particle enters the tube or the cavity with equal probability, 1/2.

B. Infinitely long connecting channels: Anomalous diffusion

As $L\to\infty$, the relaxation time in Eq. (3.12) diverges, while $D_{\rm eff}$ in Eq. (1.3) vanishes. In this limiting case, it is instructive to analyze the behavior of the mean squared displacement $\langle\Delta x^2(t|x_0)\rangle$ averaged over x_0, which we denote as $\langle\Delta x^2(t|av)\rangle$,

$$\langle \Delta x^2(t|av)\rangle = \frac{1}{l}\int_{-l/2}^{l/2} \langle \Delta x^2(t|x_0)\rangle dx_0 = 2D\int_0^t P(t')dt'. \tag{3.23}$$

Here, we have used the relations in Eqs. (1.1) and (1.5). The Laplace transform of $\langle \Delta x^2(t|av)\rangle$ is given by

$$\langle \Delta \hat{x}^2(s|av)\rangle = 2D\frac{\hat{P}(s)}{s} = \frac{2D}{s^2}\left\{1 - \hat{w}(s|av)\frac{\hat{\varphi}_{\text{tube}}(s)[1-\hat{\varphi}_{\text{de}}(s)]}{1-\hat{\varphi}_{\text{tube}}(s)\hat{\varphi}_{\text{de}}(s)}\right\}. \tag{3.24}$$

One can find the small-s behavior of this Laplace transform using Eqs. (2.8), (2.10), and (2.11). Note that when $L\to\infty$, Eq. (2.11) simplifies and takes the form

$$\hat{\varphi}_{\text{de}}(s) = \frac{1}{1+\dfrac{\sqrt{sD_{\text{ch}}}}{\kappa_{\text{ch}}}} = \frac{1}{1+\dfrac{\pi a\sqrt{sD_{\text{ch}}}}{4D}}, \tag{3.25}$$

where we have used κ_{ch} given in Eq. (2.12). Eventually, as $s\to 0$, Eq. (3.24) takes the form

$$\langle \Delta \hat{x}^2(s|av)\rangle = \frac{2D\langle \tau_{\text{tube}}\rangle \kappa_{\text{ch}}}{\sqrt{D_{\text{ch}}}s^{3/2}} = \frac{2DR^2 l}{a^2\sqrt{D_{\text{ch}}}s^{3/2}}. \tag{3.26}$$

This implies that the large-t behavior of the averaged mean squared displacement is given by

$$\langle \Delta x^2(t|av)\rangle \approx \frac{4R^2 lD}{\sqrt{\pi D_{\text{ch}}}a^2}\sqrt{t}, \quad t\to\infty. \tag{3.27}$$

Thus, in this limiting case, we have anomalous diffusion, $\langle \Delta x^2(t|av)\rangle \sim t^{\alpha}$, with the exponent $\alpha = 1/2$. Such anomalous diffusion was first discovered in studies of random walks on comblike structures with infinitely long teeth (see the book by Weiss[20] and references therein).

IV. ILLUSTRATIVE EXAMPLES

To illustrate the accuracy of our theory, we compare the theoretically predicted $\langle \Delta x^2(t|av)\rangle$ with the time dependence of the mean squared displacement averaged over x_0 obtained in Brownian dynamics simulations. This is done in Fig. 3 for the following set of the parameters: $D=1/2$, $R=l=1$, $a=0.1$, $L=0$, and $R_{\text{cav}}=2$, where R_{cav} is the cavity radius and we have assumed that the cavities are spherical. Note that for this set of parameters, D_{eff} is more than ten times smaller than D, as follows from Eq. (1.3). The theoretically predicted dependence is shown in the figure by the solid curve, while the small circles with error bars represent numerical results obtained by averaging the mean squared displacement over 5×10^4 trajectories. The theoretical curve is obtained by numerically inverting the Laplace transform of $\langle \Delta x^2(t|av)\rangle$ [Eq. (3.24)], in which functions $\hat{w}(s|av)$, $\hat{\varphi}_{\text{tube}}(s)$, and $\hat{\varphi}_{\text{de}}(s)$ are defined in Eqs. (2.8), (2.10), and (3.19), respectively. The insert in Fig. 3 shows the ratio $D(t)/D=P(t)$ obtained by numerically inverting the Laplace transform in Eq. (2.16) with the same functions $\hat{w}(s|av)$, $\hat{\varphi}_{\text{tube}}(s)$, and $\hat{\varphi}_{\text{de}}(s)$.

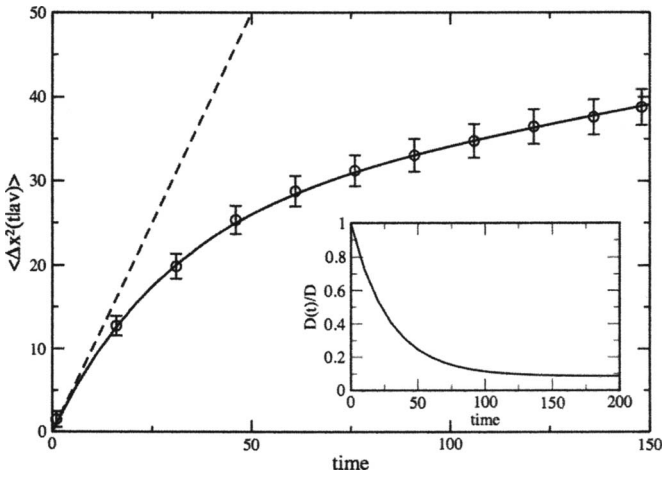

FIG. 3. The mean squared displacement of the particle averaged over the uniform distribution of its initial position in the tube as a function of time for the following set of the parameters: $D=1/2$, $R=l=1$, $a=0.1$, $L=0$, and $R_{\text{cav}}=2$. The solid curve shows the dependence obtained by numerically inverting the Laplace transform in Eq. (3.24), in which functions $\hat{w}(s|av)$, $\hat{\varphi}_{\text{tube}}(s)$, and $\hat{\varphi}_{\text{de}}(s)$ are defined in Eqs. (2.8), (2.10), and (3.19), respectively, while small circles with error bars represent the values found in Brownian dynamics simulations. The dashed line shows the mean squared displacement in the tube without dead ends. The insert shows the ratio $D(t)/D=P(t)$ obtained by numerically inverting the Laplace transform in Eq. (2.16) with the same functions $\hat{w}(s|av)$, $\hat{\varphi}_{\text{tube}}(s)$, and $\hat{\varphi}_{\text{de}}(s)$. One can see that $D_{\text{eff}}=D(\infty)$ is more than ten times smaller than D. One can also see that the expression in Eq. (4.1), leading to $\tau_{\text{rel}}\approx 30$, provides a reasonable time scale which characterizes the relaxation of $D(t)$ from D to D_{eff}.

Figure 3 shows that the theoretical curve is in excellent agreement with the numerical results. For spherical cavities of radius R_{cav}, the expression for the relaxation time in Eq. (3.15) can be written as

$$\tau_{\text{rel}} = \frac{l^2}{2D}\left(\frac{\pi}{\lambda}+\frac{1}{6}\right)\frac{4R_{\text{cav}}^3}{4R_{\text{cav}}^3+3R^2 l}. \tag{4.1}$$

In our case, $\lambda=0.1$ and τ_{rel} is about 30 dimensionless time units. From the insert, one can see that $\tau_{\text{rel}}\approx 30$ provides a reasonable time scale that characterizes relaxation of $D(t)$ from its initial value D to its asymptotic ($t\to\infty$) value D_{eff}.

In our first example, we considered the case of no connecting channels between the tube and the cavities ($L=0$). Now, we will discuss how the presence of connecting channels affects the particle diffusion in a tube with dead ends. In Fig. 4, we compare $\langle \Delta x^2(t|av)\rangle$ in structures with the same tubes and cavities but with channels of different lengths. The dependences are obtained by numerically inverting the Laplace transform in Eq. (3.24) with $\hat{w}(s|av)$, $\hat{\varphi}_{\text{tube}}(s)$, and $\hat{\varphi}_{\text{de}}(s)$ given in Eqs. (2.8), (2.10), and (2.11), respectively, for the following set of the parameters: $D_{\text{ch}}=D=1/2$, $R=l=1$, $a=0.1$, $R_{\text{cav}}=2$, where R_{cav} is the radius of the spherical cavity, and $L=0$, 500, and ∞. The results for $L=0$, 1, 3, and ∞ are shown in the insert. When $L=\infty$, the expression for $\hat{\varphi}_{\text{de}}(s)$ in Eq. (2.11) simplifies and takes the form

$$\hat{\varphi}_{\text{de}}(s) = \frac{1}{1+\dfrac{\pi a}{4}\sqrt{\dfrac{s}{D}}}. \tag{4.2}$$

All curves have the same short-time limiting behavior, $\langle \Delta x^2(t|av)\rangle = 2Dt$. Their large-$t$ asymptotic behavior is differ-

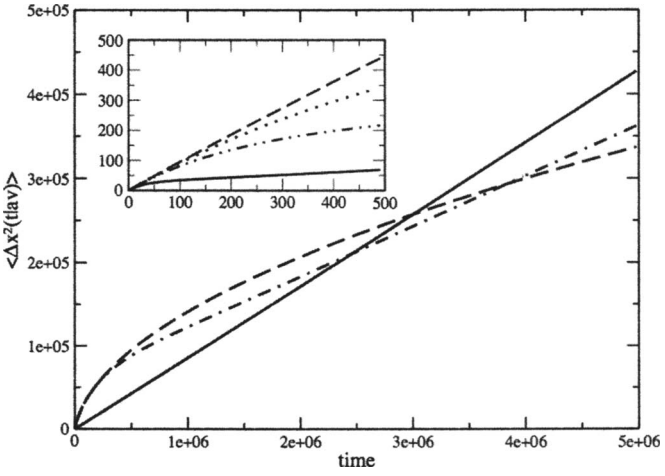

FIG. 4. The mean squared displacement of the particle averaged over the uniform distribution of its initial position in the tube as a function of time for the following set of the parameters: $D_{ch}=D=1/2$, $R=l=1$, $a=0.1$, $R_{cav}=2$, where R_{cav} is the radius of the spherical cavity, and $L=0$, 500, and ∞. The results for $L=0$, 1, 3, and ∞ are shown in the insert. The curves are obtained by numerically inverting the Laplace transform in Eq. (3.24) with $\hat{w}(s|av)$, $\hat{\varphi}_{tube}(s)$, and $\hat{\varphi}_{de}(s)$ given in Eqs. (2.8), (2.10), and (2.11), respectively. When $L=\infty$, we use $\hat{\varphi}_{de}(s)$ given in Eq. (2.11). The solid and dashed curves correspond to $L=0$ and $L=\infty$, respectively. The dashed-dotted curve corresponds to $L=500$, while the dotted and dashed-double-dotted curves in the insert correspond to $L=3$ and $L=1$, respectively. One can see that the longer the channel is, the larger the mean squared displacement in the initial stage of the process is. The reason is that the particle spends more time in the tube in systems with longer channels in the initial stage.

ent, $\langle \Delta x^2(t|av)\rangle = 2D_{eff}t$, with D_{eff} given in Eq. (1.3) for systems with finite length of the channel, and $\langle \Delta x^2(t|av)\rangle = (4R^2l/a^2)\sqrt{Dt/\pi}$ when $L=\infty$, [cf. Eq. (3.27)].

The figure shows that although the curve corresponding to $L=0$ wins at large times, it goes below the curves corresponding to nonzero length of the channel in the initial stage of the process. To rationalize this complex behavior, we note that the mean squared displacement in Eq. (3.23) can be written in terms of the mean time spent in the tube by a diffusing particle observed for time t; the particle initial position is uniformly distributed over the tube. Introducing the notation $\langle t_{tube}(t)\rangle$ for this time,

$$\langle t_{tube}(t)\rangle = \int_0^t P(t')dt', \tag{4.3}$$

we can write Eq. (3.23) as

$$\langle \Delta x^2(t|av)\rangle = 2D\langle t_{tube}(t)\rangle. \tag{4.4}$$

Based on this equation, we infer that Fig. 4 shows that the longer the channel is, the more time the particle spends in the tube in the initial stage of the process is. To explain this observation, we indicate that a particle entering a cylindrical channel of radius a and length L traverses the channel and exits on the opposite side with probability P_{tr} given by[21]

$$P_{tr} = \frac{1}{2+\dfrac{4DL}{\pi D_{ch}a}}. \tag{4.5}$$

This probability is a monotonically decreasing function of L. Thus, the larger L is, the higher the chance that a particle entering the channel from the tube returns to the tube is. This is why the particle spends more time in the tube in the initial stage of the relaxation process in the systems with longer channels.

V. COMPARISON WITH THE GKF APPROACH

In this section, we discuss the relation between our approach and the GKF approach suggested in Ref. 15. For this purpose, we consider the propagator of a particle that starts from the point $x=x_0$ located in the tube, $-\infty<x_0<\infty$, at $t=0$. At time t, this particle can be found either in the tube or in one of the dead ends. Therefore, the propagator is a two-component vector, whose components are denoted by $g_i(x,t|x_0)$, $i=1,2$. The first component, $g_1(x,t|x_0)$, is the probability density of finding the particle at point x in the tube at time t. The second component, $g_2(x,t|x_0)=g_2(nl,t|x_0)$, is the probability of finding the particle at time t in the nth dead end, and we do not specify the particle position inside the dead end. The two components satisfy

$$\frac{\partial g_1(x,t|x_0)}{\partial t} = D\frac{\partial^2 g_1(x,t|x_0)}{\partial x^2} - \sum_{n=-\infty}^{\infty}\delta(x-nl)\frac{\partial g_2(x,t|x_0)}{\partial t}, \tag{5.1}$$

$$\frac{\partial g_2(x,t|x_0)}{\partial t} = \kappa\left[g_1(x,t|x_0) - \int_0^t \varphi_{de}(t-t')g_1(x,t'|x_0)dt'\right], \tag{5.2}$$

where κ is the sink force defined in Eq. (2.1). The last term in Eq. (5.1) describes the particle transitions between the tube and the dead ends. Equation (5.2) is the conservation equation for the probability of finding the particle in the dead end located at $x=nl$.

An equivalent set of equations obtained in the framework of the GKF approach has the form

$$\frac{\partial g_1^{GKF}(x,t|x_0)}{\partial t} = D\frac{\partial^2 g_1^{GKF}(x,t|x_0)}{\partial x^2} - \frac{1}{l}\frac{\partial g_2^{GKF}(x,t|x_0)}{\partial t}, \tag{5.3}$$

$$\frac{\partial g_2^{GKF}(x,t|x_0)}{\partial t} = -\frac{\pi a^2 D_{ch}}{L}\left[\frac{g_2^{GKF}(x,t|x_0)}{V_{de}} - \frac{g_1^{GKF}(x,t|x_0)}{\pi R^2}\right]. \tag{5.4}$$

We will see that these equations are a special case of the more general Eqs. (5.1) and (5.2). The former can be recovered from the latter when (i) $\lambda = al/R^2 \ll 1$ (the weak capture regime) and (ii) the parameters of the dead end satisfy $aD_{ch} \ll LD$ and $V_{ch}=\pi a^2 L \ll V_{cav}$.

To show this, we use the fact that in the weak capture regime, the length scale associated with variation of the propagator is much greater than l on times larger than l^2/D. This allows one to reduce Eq. (5.1) to the form identical to that in Eq. (5.3). Next, we note that when the channel length satisfies $aD_{ch}/D \ll L \ll V_{cav}/a^2$, $\hat{\varphi}_{de}(s)$ in Eq. (2.11) can be approximately written as

$$\hat{\varphi}_{de}(s) \approx \frac{s(1-P_{tr})+k_{cav}P_{tr}}{s+k_{cav}P_{tr}}, \tag{5.5}$$

where P_{tr} is the translocation probability given in Eq. (4.5) which, in the case under consideration, is

$$P_{tr} \approx \frac{\pi D_{ch} a}{4DL} \ll 1. \tag{5.6}$$

Note that when $L=0$, $P_{tr}=1/2$ and Eq. (5.5) reduces to Eq. (3.19). Inverting the Laplace transform in Eq. (5.5), we obtain

$$\varphi_{de}(t) \approx (1-P_{tr})\delta(t) + k_{cav}P_{tr}^2 \exp(-k_{cav}P_{tr}t). \tag{5.7}$$

Substituting this into Eq. (5.2), we arrive at

$$\frac{\partial g_2(x,t|x_0)}{\partial t} = \kappa P_{tr}\left[g_1(x,t|x_0) - k_{cav}P_{tr} \times \int_0^t \exp[-k_{cav}P_{tr}(t-t')]g_1(x,t'|x_0)dt' \right], \tag{5.8}$$

which is identical to Eq. (5.4). One can easily see this by comparing the Laplace transforms of the two equations.

The single-exponential approximation of $\varphi_{de}(t)$ [Eq. (5.7)] is justified when the translocation probability for a particle entering the channel is small, and the time which the particle spends in the channel can be neglected. In this case, the GKF approach provides the approximation which leads to the single-exponential transient behavior of $D(t)$,

$$D_{GKF}(t) = D_{eff} + (D - D_{eff})R_{GKF}(t), \tag{5.9}$$

with

$$R_{GKF}(t) = \exp(-t/\tau_{rel}^{GKF}), \tag{5.10}$$

where the GKF relaxation time τ_{rel}^{GKF} is given by

$$\frac{1}{\tau_{rel}^{GKF}} = \left(k_{cav} + \frac{\kappa}{l}\right)P_{tr} \approx \frac{\pi a^2 D_{ch}}{L}\left(\frac{1}{V_{cav}} + \frac{1}{V_{tube}}\right). \tag{5.11}$$

To summarize, the GKF approach suggests an approximation which is applicable in the weak capture regime when the particle translocation probability through the channel is small and the time spent in the channel can be neglected. The approach fails when these conditions do not hold (for example, when $L \to 0$ or ∞). In such a situation, one has to use the more general approach based on Eqs. (5.1) and (5.2).

VI. SUMMARY

To summarize in this paper, we have analyzed the transient behavior of $D(t)$ for a particle diffusing in a tube with dead ends shown in Fig. 1. Our goal was to establish a relation between the transient behavior and the geometric parameters of the system, R, l, a, L, and V_{cav}, as well as the diffusion constants D and D_{ch}. Two main results of our analysis are given in Eqs. (2.16) and (3.12). The former gives the Laplace transform of $D(t)$ in terms of the functions $\hat{w}(s|av)$, $\hat{\varphi}_{tube}(s)$, and $\hat{\varphi}_{de}(s)$ defined in Eqs. (2.8), (2.10), and (2.11), respectively. The latter gives the relaxation time as a function of the moments, $\langle \tau_w \rangle$, $\langle \tau_{tube} \rangle$, $\langle \tau_{de} \rangle$, and $\langle \tau_{de}^2 \rangle$, which are expressed in terms of the geometric parameters and the diffusion constants in Eqs. (3.5), (3.11), and (3.13), respectively.

ACKNOWLEDGMENTS

A.M.B. is grateful to Attila Szabo for numerous enlightening discussions of different questions related to the problem. L.D. thanks CONACyT for partial support by Grant No. 52305. Two of the authors (Yu. A. M. and V. Yu. Z.) thank the Russian Foundation of Basic Research for support (Grant No. 06-03-32373). This study was partially supported by the Intramural Research Program of the NIH, Center for Information Technology.

APPENDIX A: DERIVATION OF Eq. (2.8)

Consider a particle diffusing on the interval of length $l/2$, $0<x<l/2$, terminated by an absorbing endpoint at $x=0$ and reflecting endpoint at $x=l/2$. The particle starts from $x=x_0$, and its propagator $G(x,t|x_0)$ satisfies the diffusion equation

$$\frac{\partial G}{\partial t} = D\frac{\partial^2 G}{\partial x^2}, \quad 0<x<l/2, \tag{A1}$$

the initial condition $G(x,0|x_0)=\delta(x-x_0)$, and the boundary condition

$$G(0,t|x_0) = \left.\frac{\partial G(x,t|x_0)}{\partial x}\right|_{x=l/2} = 0. \tag{A2}$$

The probability density for the particle lifetime, which is the probability density for its first passage time to the absorbing boundary, $w(t|x_0)$ is given by

$$w(t|x_0) = D\left.\frac{\partial G(x,t|x_0)}{\partial x}\right|_{x=0}. \tag{A3}$$

To find the Laplace transform of $w(t|x_0)$, we first find the Laplace transform of the propagator by solving Eq. (A1) in the Laplace space. Then, using the definition in Eq. (A3), we obtain

$$\hat{w}(s|x_0) = \frac{\cosh\left(\left(\frac{l}{2}-x_0\right)\sqrt{\frac{s}{D}}\right)}{\cosh\left(\frac{l}{2}\sqrt{\frac{s}{D}}\right)}. \tag{A4}$$

Averaging this expression over the starting points x_0, $0<x_0<l/2$, we arrive at the expression in Eq. (2.8).

APPENDIX B: DERIVATION OF Eq. (2.10)

Consider a particle diffusing on the interval of length l, $-l/2<x<l/2$, terminated by reflecting endpoints at $x=\pm l/2$. The interval contains a delta sink of the strength κ located at the origin. The particle starts from the origin, $x=0$, and its propagator $G(x,t)$ satisfies the diffusion equation

$$\frac{\partial G}{\partial t} = D\frac{\partial^2 G}{\partial x^2} - \kappa\delta(x)G, \quad -l/2 < x < l/2, \tag{B1}$$

the initial condition $G(x,0)=\delta(x)$, and the boundary condition

$$\left.\frac{\partial G(x,t)}{\partial x}\right|_{x=\pm l/2} = 0. \tag{B2}$$

The probability density for the particle lifetime in the tube $\varphi_{\text{tube}}(t)$ is given by

$$\varphi_{\text{tube}}(t) = \kappa G(0,t). \tag{B3}$$

To find the Laplace transform of $\varphi_{\text{tube}}(t)$ given in Eq. (2.10), we first find the Laplace transform of the propagator $\hat{G}(0,s)$ by solving Eq. (B1) in the Laplace space, and then use the definition in Eq. (B3).

APPENDIX C: DERIVATION OF Eq. (2.11)

Consider a particle entering a dead end channel from the tube at $t=0$. We take that the channel is parallel to the z axis, and its exits at $z=0$ and L, connects the channel with the tube and cavity, respectively. If the particle does not escape from the dead end for time t, it can be found either in the channel or in the cavity. Therefore, the particle propagator in the dead end is a two-component vector: Its first component, $G(z,t)$, is the probability density of finding the particle at point z of the channel at time t, while the second component, $P(t)$, is the probability of finding the particle in the cavity. The two components satisfy

$$\frac{\partial G}{\partial t} = D_{\text{ch}}\frac{\partial^2 G}{\partial z^2} - \delta(z-L)[\kappa_{\text{ch}}G - k_{\text{cav}}P], \quad 0 < z < L, \tag{C1}$$

$$\frac{dP(t)}{dt} = -k_{\text{cav}}P(t) + \kappa_{\text{ch}}G(L,t), \tag{C2}$$

the initial conditions $G(z,0)=\delta(z)$, $P(0)=0$, and the boundary conditions

$$D_{\text{ch}}\left.\frac{\partial G(z,t)}{\partial z}\right|_{z=0} = \kappa_{\text{ch}}G(0,t), \quad \left.\frac{\partial G(z,t)}{\partial z}\right|_{z=L} = 0. \tag{C3}$$

The probability density for the particle lifetime in the dead end $\varphi_{\text{de}}(t)$ is given by

$$\varphi_{\text{de}}(t) = \kappa_{\text{ch}}G(0,t). \tag{C4}$$

To find the Laplace transform of $\varphi_{\text{de}}(t)$ given in Eq. (2.11), we first find the Laplace transform of $G(0,t)$ by solving Eqs. (C1) and (C2) in the Laplace space, and then use the definition in Eq. (C4).

[1] P. S. Bressloff and B. A. Earnshow, Phys. Rev. E **75**, 041915 (2007).
[2] F. Santamaria, S. Wils, E. De Schutter, and G. J. Augustine, Neuron **52**, 635 (2006).
[3] A. Tao, L. Tao, and C. Nicholson, J. Theor. Biol. **234**, 525 (2005).
[4] L. Tao and C. Nicholson, J. Theor. Biol. **229**, 59 (2004).
[5] J. Hrabe, S. Hrabetova, and K. Segeth, Biophys. J. **87**, 1606 (2004).
[6] S. Hrabetova and C. Nicholson, Neurochem. Int. **45**, 467 (2004).
[7] S. Hrabetova, J. Hrabe, and C. Nicholson, J. Neurosci. **23**, 8351 (2003).
[8] R. E. Safford, E. A. Bassingthwaighte, and J. B. Bassingthwaighte, J. Gen. Physiol. **72**, 513 (1978).
[9] M. Suenson, D. R. Richmond, and J. B. Bassingthwaighte, Am. J. Physiol. **227**, 1116 (1974).
[10] E. Page and R. S. Bernstein, J. Gen. Physiol. **47**, 1129 (1964).
[11] A. Pinner and P. H. Nye, Eur. J. Soil. Sci. **33**, 25 (1982).
[12] P. S. C. Rao, R. E. Jessup, and T. M. Addiscott, Soil Sci. **133**, 342 (1982).
[13] J. R. Philip, Austral. J. Soil Res. **6**, 1 (1968).
[14] J. R. Philip, Austral. J. Soil Res. **6**, 21 (1968).
[15] R. C. Goodknight, W. A. Klikoff, and I. Fatt, J. Phys. Chem. **64**, 1162 (1960).
[16] P. N. Sen, L. M. Schwartz, P. P. Mitra, and B. I. Halperin, Phys. Rev. B **49**, 215 (1994).
[17] L. Dagdug and A. M. Berezhkovskii, J. Chem. Phys. **125**, 244705 (2006).
[18] I. V. Grigoriev, Yu. A. Makhnovskii, A. M. Berezhkovskii, and V. Yu. Zitserman, J. Chem. Phys. **116**, 9574 (2002).
[19] S. M. Bezrukov, A. M. Berezhkovskii, M. A. Pustovoit, and A. Szabo, J. Chem. Phys. **113**, 8206 (2000).
[20] G. H. Weiss, *Aspects and Applications of the Random Walk* (North-Holland, Amsterdam, 1994).
[21] A. M. Berezhkovskii, M. A. Pustovoit, and S. M. Bezrukov, J. Chem. Phys. **116**, 9952 (2002).